Stochastic dynamic stability analysis of composite curved panels subjected to non-uniform partial edge loading

S. Dey, T. Mukhopadhyay, S.K. Sahu, S. Adhikari

PII: S0997-7538(16)30225-X

DOI: 10.1016/j.euromechsol.2017.09.005

Reference: EJMSOL 3490

To appear in: *European Journal of Mechanics / A Solids*

Received Date: 5 September 2016

Revised Date: 17 September 2017

Accepted Date: 18 September 2017

Please cite this article as: Dey, S., Mukhopadhyay, T., Sahu, S.K., Adhikari, S., Stochastic dynamic stability analysis of composite curved panels subjected to non-uniform partial edge loading, *European Journal of Mechanics / A Solids* (2017), doi: 10.1016/j.euromechsol.2017.09.005.

S. Dey [1], T. Mukhopadhyay [2,*], S. R. Sahu [3], S. Adhikari [2]

[1] Mechanical Engineering Department, National Institute of Technology Silchar, India

[2] College of Engineering, Swansea University, United Kingdom

[3] Department of Civil Engineering, National Institute of Technology Rourkela, India

Abstract

The stochastic dynamic stability analysis of laminated composite curved panels under non-uniform partial edge loading is studied using finite element analysis. The system input parameters are randomized to ascertain the stochastic first buckling load and zone of resonance. Considering the effects of transverse shear deformation and rotary inertia, first order shear deformation theory is used to model the composite doubly curved shells. The stochasticity is introduced in Love's and Donnell's theory considering dynamic and shear deformable theory according to the Sander's first approximation by tracers for doubly curved laminated shells. The moving least square method is employed as a surrogate of the actual finite element model to reduce the computational cost. The results are compared with those available in the literature. Statistical results are presented to show the effects of radius of curvatures, material properties, fibre parameters, and non-uniform load parameters on the stability boundaries.

Keywords: Composite curved panel; Stochastic dynamic stability; Moving least square method

[*] Corresponding author: *Tanmoy Mukhopadhyay, E-mail: 800712@swansea.ac.uk*

decades for the design of structures in aerospace, automotive, civil and other engineering applications. It has improved the performance and reliability of structural system due to its mechanical advantages of specific modulus and specific strength over monolithic materials, improved fatigue, impact resistance, and design flexibility. Such structures subjected to in-plane periodic forces may lead to parametric resonance because of certain random combinations in the values of uncertain parameters. The instability may occur below the stochastic critical load of the structure under compressive loads over wide ranges of resonance frequencies. Specially the aerospace structures such as skin panels in wings, fuselage, submarine hulls and civil application has practical importance of stability analysis of doubly curved panels/open shells subjected to uncertain non-uniform loading condition. Traditionally, structural analysis is formulated with deterministic behavior of material properties, loads and other system parameters. However, the real-life structures employed in aerospace, naval, civil, and mechanical applications are always subjected to intrusive uncertainties. The inherent sources of such uncertainties in real structural problems can be due to randomness in material properties, loading conditions, geometric properties and other random input parameters. As an inevitable consequence of the uncertainties in these system parameters, the response of structural system will always exhibit some degree of uncertainty. The traditional deterministic analysis based on an exact reliable model would not help in properly accounting the variation in the response and therefore, the analysis based on deterministic material properties may vary significantly from the real behaviour. The incorporation of randomness of input parameters enables the prediction of the performance variation in the presence of uncertainties and more importantly their sensitivity for targeted testing and quality control. In order to provide useful and accurate information about the safe

putational technologies in recent years has led to high-resolution numerical models of real-life engineering structural systems. It is also required to quantify uncertainties and robustness associated with a computational model. Hence, the quantification of uncertainties plays a key role in establishing the credibility of a numerical model. Therefore, the development of an efficient mathematical model possessing the capability to quantify the uncertainties present in the structures is extremely essential in order to accurately assess the laminated composite structures.

Structural elements under in-plane periodic forces may undergo unstable transverse vibrations, leading to parametric resonance, due to certain combinations of the values of in-plane load parameters and natural frequency of transverse vibration. Several means of combating parametric resonance such as damping and vibration isolation may be inadequate and sometimes dangerous with reverse results (Evan-Iwanowski, 1965). A number of catastrophic incidents can be traced to parametric instability and is often studied in the spectrum of determination of natural frequency and critical load of structures. The stochasticity in the measurement of natural frequencies, critical load and ultimately the excitation frequencies during parametric resonance are of great technical importance in studying the instability behavior of dynamic systems. Many authors addressed the parametric instability characteristics of laminated composite flat panel subjected to uniform loads (Iwatsubo et al., 1973; Moorthy and Reddy, 1990; Chen and Yang, 1990; Patel et al., 2009; Kochmann and Drugan, 2009; Singha and Daripa, 2009; Kim et al., 2013). In contrast, Bolotin (1964) and Yao (1965) studied the parametric resonance subjected to periodic loads. Stochastic principal parametric resonance of composite laminated beam is numerically investigated by Lan et al. (2014). The influences of transverse shear (Andrzej et al., 2011)

composite beam (Meng-Kao and Yao, 2004), plates (Dey and Singha, 2006) or shells (Bert and Birman, 1988) and stiffened panel (Sepe et al., 2016). Further studies are also carried out for modelling mesoscopic volume fraction stochastic fluctuations in fiber reinforced composites (Guilleminot et al., 2008) and for parametric instability of graphite-epoxy composite beams under excitation (Yeh and Kuo, 2004). Free vibration and dynamic stability analysis of rotating thin-walled composite beams (Saraviaa et al., 2011) and nonlinear thermal stability of eccentrically stiffened functionally graded truncated conical shells are recently reported (Duc and Cong, 2015). In contrast, many numerical investigations are carried out using response surface methods such as moving least square (MLS) method and other methods for structural analysis (Choi et al., 2004; Wu et al., 2005; Park and Grandhi, 2014; Shu et al., 2007; Kang et al., 2010). Some researchers studied specifically on the moving least squares (MLS) approximation for the regression analysis (Lancaster and Salkauskas, 1981; Breitkpf et al., 2005) instead of the conventional least squares (LS) approximation in conjunction to traditional response surface method (RSM) techniques (Mukhopadhyay et al., 2015, Dey et al., 2015a). Several studies are carried out on uncertainty quantification for dynamic response of structures including different surrogate based analyses of composite beams, plates and shells (Sarrouy et al., 2013; Dey et al., 2015(b-d), 2016(a-f), 2018; Mukhopadhyay et al.,2016; Naskar et al.,2017). Few articles have reported the critical comparative assessment of different surrogate models for their performance in dynamic analyses of composite laminates (Dey et al.,2017; Mukhopadhyay et al.,2017).

To the best of authors' knowledge, no literature is reported on uncertainty quantification of parametric instability of doubly curved composite shells. The application of stochastic

region (DSR). Thus it is imperative to consider the effect of stochasticity for robust analysis, design and control of the system. The application of moving least square method in this realm as a computationally efficient surrogate of expensive finite element method has not been investigated yet. Even though the perturbation method is an efficient way of stochastic analysis for relatively simpler structures (Kaminski, 2013; Gadade et al., 2016), this intrusive method can be mathematically quite cumbersome for complex problems like stochastic dynamic stability analysis of composite laminates. The main drawback of this method is that it can obtain only the statistical moments (not the entire probability distribution) of the stochastic output quantity of interest. If the nature of the output distribution is known to be Gaussian, the probability distribution can be obtained using the first two moments. However, the nature of distribution of the output parameter may not be known a priori in most engineering problems. Monte Carlo simulation, on the other hand, can obtain the entire probabilistic description of the stochastic output parameter. The main lacuna of traditional Monte Carlo simulation is its computational intensiveness. A surrogate based Monte Carlo simulation approach, as followed in this paper, allows us to quantify the probabilistic descriptions in a computationally efficient manner. In the present study, a moving least square based approach is employed in conjunction with finite element formulation to figure out the random eigenvalue problem and quantify the probabilistic characteristics of the responses related to dynamic stability of composite laminates. The numerical results are shown for first random buckling load and stochastic fundamental resonance frequencies with individual and combined variation of the stochastic input parameters.

2. Importance of stochastic dynamic stability analysis in composite laminates

unbalanced inertia force, bridges are frequently subjected to the cyclic loads from the running vehicles, marine structures are always suffered the periodic wave forces etc. Structural components subjected to in-plane periodic forces undergo an unstable dynamic response known as dynamic instability or parametric instability or parametric resonance. Parametric resonance, may occur for certain combinations of natural frequency of transverse vibration, the frequency of the in-plane forcing functions and the magnitude of the in-plane load. A number of flight accidents can be traced due to parametric instability of structures. In comparison to the principal resonance, the parametric instability can take place not only at a single excitation frequency but even for small excitation amplitudes and combination of frequencies. The difference between good and bad vibration regimes of a structure under in-plane periodic loads can be found from dynamic instability region (DIR) spectra. The computation of these spectra is usually studied in term of natural frequencies and static buckling loads. The parametric instability has a catastrophic effect on structures near critical regions of parametric instability. Hence, the parametric resonance characteristics of structures are of great technical importance for understanding the dynamic characteristics under periodic loads.

As discussed in the preceding paragraph, structures are subjected to dynamic loads more often than static loads. Dynamic load means the load varies with time. Periodic loading is one type of dynamic loading. This type of load occurs in repeated periods or cycles like sine and cosine functions. Structures subjected to in-plane periodic loads can be expressed in the form as suggested by Bolotin (1964) : $P(t) = P_s + P_t \cos\Omega t$, where P_s is the static portion of $P(t)$, P_t is the amplitude of the dynamic portion of $P(t)$ and Ω is the frequency of excitation. It can be noted here that the quantities P_s, P_t, Ω possess random values in practical

other sources of stochasticity for a comprehensive probabilistic analysis of the system. Laminated composites being a complex structural form and susceptible to different forms of uncertainty, the compound effects of stochastic time varying loading and structural and material uncertainties associated with composites can be crucial in the intended performance for various engineering applications.

3. Governing equations

In the present study, a layered graphite-epoxy composite laminated simply supported shallow doubly curved shell is considered with thickness *t*, intensity of loading *C*, principal radii of curvature R_x , R_y along x- and y-direction, respectively and the radius of curvature R_{xy} in x-y plane, as furnished in Figure 1. Using Hamilton's principle (Meirovitch, 1992) for free vibration of composite shell structure subjected to in-plane loads, the equation of equilibrium can be expressed as

$$[M(\tilde{\omega})][\ddot{q}] + ([K_e(\tilde{\omega})] - F(\tilde{\omega})[K_g(\tilde{\omega})])\{q\} = 0 \tag{1}$$

where $M(\tilde{\omega})$, $K_e(\tilde{\omega})$ and $K_g(\tilde{\omega})$ are mass, elastic stiffness and geometric stiffness matrices, respectively. Here $\tilde{\omega}$ is used to denote the element of probability space. Therefore, any quantity expressed as a function of $\tilde{\omega}$ is a random quantity (can be a scalar, vector or a matrix). The in-plane load $[F(\tilde{\omega})(t)]$ is periodic and can be expressed in the stochastic form (Patel et al., 2009)

$$F(\tilde{\omega})(t) = F_s(\tilde{\omega}) + F_t(\tilde{\omega})Cos\Omega t \tag{2}$$

where $F_s(\tilde{\omega})$ and $F_t(\tilde{\omega})$ are the random static portion and the amplitude of the dynamic portion of stochastic in-plane load, respectively. The static buckling load of elastic shell $F_{cr}(\tilde{\omega})$ is the measure of the magnitude of $F_s(\tilde{\omega})$ and $F_t(\tilde{\omega})$

equation of motion can be expressed by employing equation (2) as

$$[M(\tilde{\omega})][\ddot{q}] + ([K_e(\tilde{\omega})] - \alpha(\tilde{\omega})\, F_{cr}(\tilde{\omega})[K_g(\tilde{\omega})] - \beta(\tilde{\omega})\, F_{cr}(\tilde{\omega})[K_g(\tilde{\omega})]\cos\Omega t\,)\{q\} = 0 \qquad (4)$$

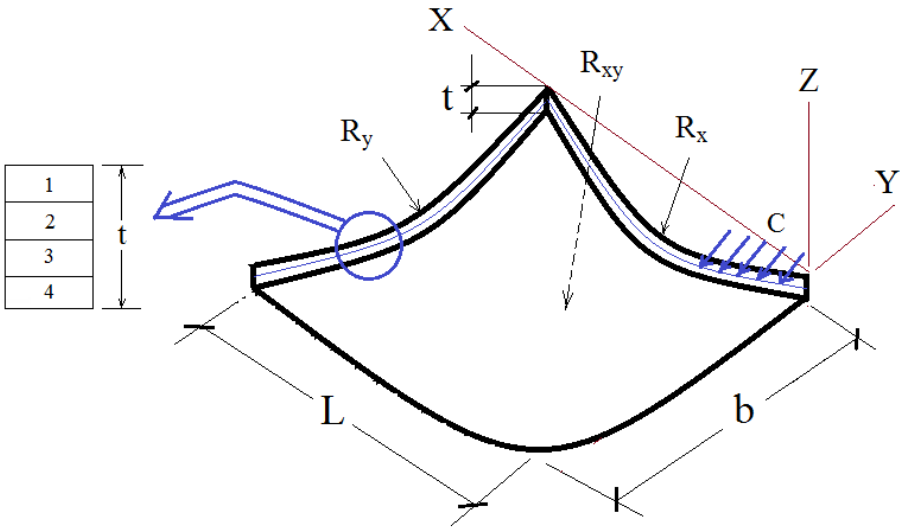

Fig. 1 Laminated composite curved panel

It can be noted that the matrices involved in equation (4) are stochastic in nature. Depending on the degree of stochasticity, each element of the matrices is random in nature. The solution of equation (4) would obtain different results for each of the realizations of a Monte Carlo simulation depending on the respective set of input parameters. Thus probabilistic distributions can be obtained based on the results of different realizations following a non-intrusive method. This stochastic equation (4) indicates second order differential equations with periodic Mathieu-Hill type coefficients. The formation of zone of instability arises from Floquet's theory which establishes the existence of periodic solutions. The periodic solutions of period T and $2T$ derive the limiting bounds of the dynamic instability regions (where $T = 2\pi/\Omega$). The significant stochastic importance lies in the limiting bounds of primary instability regions with period $2T$ (Chen and Yang, 1990) wherein the solution can be represented as the trigonometric series form

expressed by equating the coefficients of $Sin(\Omega t/2)$ and $Cos(\Omega t/2)$ as

$$\left[[K_e(\tilde{\omega})] - \alpha(\tilde{\omega})\, F_{cr}(\tilde{\omega})[K_g(\tilde{\omega})] \pm \beta(\tilde{\omega})\, F_{cr}(\tilde{\omega})[K_g(\tilde{\omega})] - \frac{\Omega^2}{4}[M]\right]\{q\} = 0 \qquad (6)$$

The above equation (6) represents an eigenvalue problem for known values of $\alpha(\tilde{\omega})$, $\beta(\tilde{\omega})$ and $F_{cr}(\tilde{\omega})$ as for $\Omega_j q_j = 0$ for j=1,2,3…. Here the two conditions under a plus and minus sign represents the two limiting bounds of the dynamic instability region. The eigenvalues (Ω_j) provide the boundary frequencies of the instability regions for specific values of α and β and the reference stochastic static buckling load is computed accordingly (Ganapathi et al., 1999) and in contrast, exact solution for doubly curved shells can also be carried out (Chaudhuri and Abuarja, 1988). An eight-noded curved isoparametric element is employed with five degrees of freedom u, v, w, θ_x and θ_y per node. The present study employs the first order shear deformation theory and the shear correction coefficient for the nonlinear distribution of the thickness shear strains through the total thickness. The displacement field along mid-plane is assumed to be straight before and after deformation, but it is not necessary to remain normal after deformation. The displacement components can be expressed as

$$\begin{aligned} \bar{u}(x, y, z) &= u(x, y) + z\,\theta_x(x, y) \\ \bar{v}(x, y, z) &= v(x, y) + z\,\theta_y(x, y) \\ \bar{w}(x, y, z) &= w(x, y) \end{aligned} \qquad (7)$$

where the rotations of the mid-plane surface are represented by θ_x and θ_y. Here the displacement components in the *x*, *y*, *z* directions at any point and at the mid-plane surface are denoted as $\bar{u}$, $\bar{v}$, $\bar{w}$, and u, v and w, respectively. Thus the integrated relationship for the composite curved shell can be represented as

where A_{ij}, B_{ij}, D_{ij} (where i, j=1,2,6) and S_{ij} (where i, j=4,5) are the extension-bending coupling, bending and transverse shear stiffness, respectively. The shear correction factor (=5/6) is incorporated in S_{ij} in the numerical calculation. In the present analysis, shear deformable Sander's kinematic relation (Bathe, 1990) is extended for doubly curved shells. The strain displacement equations of linear nature can be obtained as

$$\varepsilon_{xl}(\tilde{\omega}) = \frac{\partial u}{\partial x} + \frac{w}{R_x(\tilde{\omega})} + z\kappa_x$$

$$\varepsilon_{yl}(\tilde{\omega}) = \frac{\partial v}{\partial y} + \frac{w}{R_y(\tilde{\omega})} + z\kappa_y$$

$$\gamma_{xyl}(\tilde{\omega}) = \frac{\partial u}{\partial y} + \frac{\partial v}{\partial x} + z\kappa_{xy} \tag{9}$$

$$\gamma_{yz}(\tilde{\omega}) = \frac{\partial w}{\partial y} + \theta_y - C_1\frac{v}{R_y(\tilde{\omega})}$$

$$\gamma_{xz}(\tilde{\omega}) = \frac{\partial w}{\partial x} + \theta_x - C_1\frac{u}{R_x(\tilde{\omega})}$$

where

$$\kappa_x = \frac{\partial \theta_x}{\partial x} \quad \text{and} \quad \kappa_y = \frac{\partial \theta_y}{\partial y}$$

$$\kappa_{xy}(\tilde{\omega}) = \frac{\partial \theta_x}{\partial y} + \frac{\partial \theta_y}{\partial x} + \frac{1}{2}C_2\left(\frac{1}{R_x(\tilde{\omega})} - \frac{1}{R_y(\tilde{\omega})}\right)\left(\frac{\partial v}{\partial x} - \frac{\partial u}{\partial y}\right) \tag{10}$$

Here the formulation can be derived to shear deformable Love's first approximation and Donnell's theories from tracers (C_1 and C_2). Considering nonlinearity in strain, the element geometric stiffness matrix for doubly curved shells can be expressed as

$$\varepsilon_{xnl}(\tilde{\omega}) = \frac{1}{2}\left(\frac{\partial u}{\partial x} + \frac{w}{R_x(\tilde{\omega})}\right)^2 + \frac{1}{2}\left(\frac{\partial v}{\partial x}\right)^2 + \frac{1}{2}\left(\frac{\partial w}{\partial x} - \frac{u}{R_x(\tilde{\omega})}\right)^2 + \frac{1}{2}z^2\left[\left(\frac{\partial \theta_x}{\partial x}\right)^2 + \left(\frac{\partial \theta_y}{\partial x}\right)^2\right] \tag{11}$$

$$\gamma_{xynl}(\tilde{\omega})=\left[\left(\frac{\partial u}{\partial x}+\frac{w}{R_x(\tilde{\omega})}\right)\frac{\partial u}{\partial y}+\left(\frac{\partial v}{\partial y}+\frac{w}{R_y(\tilde{\omega})}\right)\frac{\partial v}{\partial x}+\left(\frac{\partial w}{\partial x}-\frac{u}{R_x(\tilde{\omega})}\right)\left(\frac{\partial w}{\partial y}-\frac{v}{R_y(\tilde{\omega})}\right)\right]$$
$$+\ z^2\left[\left(\frac{\partial \theta_x}{\partial x}\right)\left(\frac{\partial \theta_x}{\partial y}\right)+\left(\frac{\partial \theta_y}{\partial x}\right)\left(\frac{\partial \theta_y}{\partial y}\right)\right]$$

The overall stochastic stiffness and mass matrices i.e., $[K_e(\tilde{\omega})]$, $[K_g(\tilde{\omega})]$ and $[M(\tilde{\omega})]$ are obtained by assembling the corresponding element matrices by using skyline technique. The element mass and stiffness matrices of composite shells are computed wherein the geometric stiffness matrix is obtained as the function of in-plane stress distribution in the element due to applied edge loading. Due to non-uniformity in the stress field, plane stress analysis is carried out by using the finite element formulation. The possible shear locking is avoided by employing the reduced integration technique for the element matrices. The subspace iteration method (Bathe, 1990) is utilized to solve the stochastic eigenvalue problems.

4. Moving least square method

In general, the polynomial regression models give the large errors in conjunction to non-linear responses while give good approximations in small regions wherein the responses are less complex. Such features are found advantageous while implementing the method of moving least squares (MLS). Moreover, the least square method gives a good result to represent the original limit state but it creates a problem if anyone like to fit a highly nonlinear limit function with this technique because this technique uses same factor for approximation throughout the space of interest. To overcome this problem, the moving least square method is introduced. In this method, a weighted interpolation function or limit state function is employed to the response surface and some extra support points are also generated

$x = [x_1, x_2, x_3, ...x_n]^T$, characterized by a probability density function (PDF) with a particular distribution such as normal or lognormal with limit state function of these random variables. To avoid the curse of dimensionality in dealing with random input variables, response surface methods (RSM) can be utilised to increase the computational efficiency. These methods approximate an implicit limit state function as a response surface function (RSF) in an explicit form, which is evaluated for a set of selected design points throughout a number of deterministic structural analyses. RSM approximates an implicit limit state function as a RSF in explicit form. It selects experimental points by an axial sampling scheme and fits these experimental points using a second order polynomial without cross terms expressed as

$$y(x) = \beta_o + \sum_{i=1}^{k} \beta_i \; x_i + \sum_{i=1}^{k} \sum_{j>i}^{k} \beta_{ij} \; x_i \; x_j + \sum_{i=1}^{k} \beta_{ii} \; x_i^2 \tag{12}$$

where β_o, β_i, β_{ij} and β_{ii} are the unknown coefficients of the polynomial equation. The least squares approximation commonly used in the conventional RSM allots equal weight to the experimental points in evaluating the unknown coefficients of the RSF. The weights of these experimental points should consider the proximity to the actual limit state function so that MLS enables a higher weight to yield a more accurate output. The approximated RSF can be defined in terms of basis functions $b(x)$ and the coefficient vector $a(x)$ as

$$\tilde{L}(x) = b(x)^T \; a(x) \tag{13}$$

The coefficient vector $a(x)$ is expressed as a function of the random variables x to consider the variation of the coefficient vector according to the change of the random variable at each iteration. The local MLS approximation at x is formulated as (Kang et al., 2010)

$$b(x) = \left[1\, x_1 \ldots\ldots x_n\, x^2 \ldots\ldots x_n^2\right]^T \tag{15}$$

The vector of unknown coefficients $a(x)$ is determined by minimizing the error between the experimental and approximated values of the limit state function. This error is defined as

$$Err(x) = \sum_{i=1}^{n} w(x - x_i)\left[\tilde{L}(x, x_i) - L(x_i)\right]^2 = (Ba - L)^T\, W(x)\,(Ba - L) \tag{16}$$

where $L = \left[L(x_1), L(x_2), \ldots\ldots\ldots L(x_n)\right]^T$, $B = \left[b(x_1), b(x_2), \ldots\ldots\ldots b(x_n)\right]^T$ and $W(x) = diag.\left[w_1(x_1 - x), w_2(x_2 - x), \ldots\ldots\ldots w_m(x_n - x)\right]$. Here ($n$+1) is the number of sampling points and (m+1) is the number of basis functions. Now for minimization of error with respect to $a(x)$, $\partial(Err)/\partial a = 0$ transforming the coefficient of vector $a(x)$ as

$$a(x) = (B^T\, W(x)\, B)^{-1}\, B^T\, W(x)\, L \tag{17}$$

The approximated response surface function is obtained from equation (14) as

$$\tilde{L}(x) = b(x)^T\, (B^T\, W(x)\, B)^{-1}\, B^T\, W(x)\, L \tag{18}$$

5. Random input representation

The random input parameters such as ply-orientation angle, radius of curvatures, material properties (both longitudinal and transverse elastic modulus, shear modulus, Poisson ratio, mass density), load, load factors (both static and dynamic) and combined variation of all these parameters are considered for composite doubly curved shells considering layer-wise stochasticity. It is assumed that the uniform random distribution of input parameters exists within a certain band of tolerance with their mean values. The following cases are considered in the present study:

(a) Variation of ply-orientation angle only: $\theta(\tilde{\omega}) = \{\theta_1\ \theta_2\ \theta_3 \ldots\ldots\ldots \theta_i \ldots\ldots \theta_l\}$

$P(\tilde{\omega}) = \{E_1(\tilde{\omega}), E_2(\tilde{\omega}), G_{12}(\tilde{\omega}), G_{23}(\tilde{\omega}), G_{13}(\tilde{\omega}), \mu(\tilde{\omega}), \rho(\tilde{\omega})\}$

(d) Variation of intensity of load only: $\{F(\tilde{\omega})\}$

(e) Variation of static load factor $\{\alpha(\tilde{\omega})\}$ and dynamic load factor $\{\beta(\tilde{\omega})\}$

(f) Combined variation of ply orientation angle, radius of curvatures, material properties (namely, elastic moduli, shear moduli, Poisson's ratio and density), applied load and load factors (static and dynamic): $\{\theta, R, P, F, \alpha, \beta\}(\tilde{\omega})$

In the present study, $\pm 5^{o}$ variation for ply orientation angle, $\pm 10\%$ volatility in material properties (as per industry standard), applied load and load factors, respectively are considered from their respective deterministic values unless otherwise specified. Figure 2 presents a flowchart of the stochastic dynamic stability analysis using MLS method (surrogate based Monte Carlo simulation) as followed in the present study. A brief description of the Monte Carlo simulation method is provided in the following paragraphs.

Uncertainty quantification is part of modern structural analysis problems. Practical structural systems are faced with uncertainty, ambiguity, and variability constantly. Even though one might have unprecedented access to information due to the recent improvement in various technologies, it is impossible to accurately predict future structural behaviour during its service life. Monte Carlo simulation, a computerized mathematical technique, lets us realize all the possible outcomes of a structural system leading to better and robust designs for the intended performances. The technique was first used by scientists working on the atom bomb; it was named after Monte Carlo, the Monaco resort town renowned for its casinos. Since it's introduction in World War II, this technique has been used to model a variety of physical and conceptual systems across different fields such as engineering,

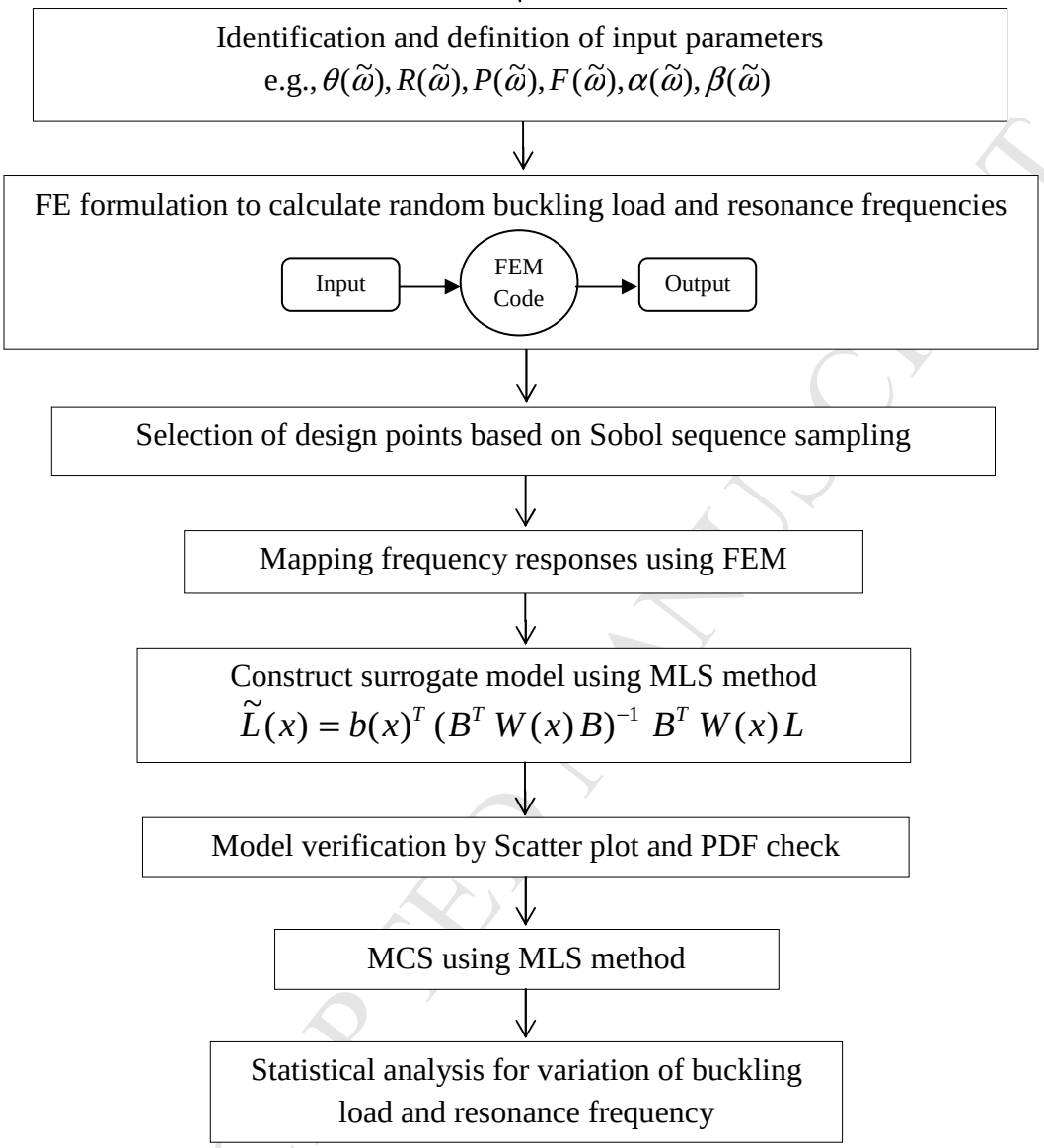

Fig. 2 Flowchart of stochastic dynamic stability analysis using MLS method

finance, project management, energy, manufacturing, research and development, insurance, oil and gas, transportation and environment.

Monte Carlo simulation furnishes a range of prospective outcomes along with their respective probability of occurrence. This technique performs uncertainty quantification by forming probabilistic models of all possible results accounting a range of values from the probability distributions of any factor that has inherent uncertainty. It simulates the outputs

Monte Carlo simulation could involve thousands or tens of thousands of recalculations before it can provide a converged result depicting the distributions of possible outcome values of the response quantities of interest. Each set of samples is called an iteration or realization, and the resulting outcome from that sample is recorded. In this way, Monte Carlo simulation provides not only a comprehensive view of what could happen, but how likely it is to happen i.e. the probability of occurrence.

The mean or expected value of a function $f(x)$ of a *n* dimensional random variable vector, whose joint probability density function is given by (x), can be expressed as

$$\mu_f = E\left[f(x) \right] = \int_{\Omega} f(x) \phi(x)\, dx \tag{19}$$

Similarly the variance of the random function $f(x)$ is given by the integral below,

$$\sigma_f^2 = Var\left[f(x) \right] = \int_{\Omega} \left(f(x) - \mu_f \right)^2 \phi(x)\, dx \tag{20}$$

The above multidimensional integrals, as shown in equation (19) and (20) are difficult to evaluate analytically for many types of joint density functions and the integrand function $f(x)$ may not be available in analytical form for the problem under consideration. Thus the only alternative way is to calculate it numerically. The above integral can be evaluated using MCS approach, wherein *N* sample points are generated using a suitable sampling scheme in the *n*-dimensional random variable space. The *N* samples drawn from a dataset must follow the distribution specified by $\varphi(x)$. Having the *N* samples for *x*, the function in the integrand $f(x)$ is evaluated at each of the *N*-sampling points x_i of the sample set $\chi = \{x_1, ..., x_N\}$. Thus, the integral for the expected value takes the form of averaging operator as shown below

Similarly, using sampled values of MCS, the equation (20) leads to

$$\sigma_f^2 = Var\left[f(x) \right] = \frac{1}{N-1} \sum_{i-1}^{N} \left(f(x_i) - \mu_f \right)^2 \tag{22}$$

Thus the statistical moments can be obtained using a brute force Monte Carlo simulation based approach, which is often computationally very intensive due the evaluation of function $f(x_i)$ corresponding to the *N*-sampling points x_i, where $N \sim 10^3$. The noteworthy fact in this context is the adoption of surrogate based Monte Carlo simulation approach in the present study that reduces the computational burden of traditional (i.e. brute force) Monte Carlo simulation to a significant extent.

6. Results and Discussion

The present study considers a simply supported four layered graphite-epoxy angle-ply (45°/-45°/45°/-45°) and cross-ply (0°/90°/0°/90°) composite doubly curved shallow shells. In finite element formulation, an eight noded isoparametric quadratic element is considered. For graphite-epoxy composite shells, the deterministic values of geometric properties are considered as L = 1 m, b = 0.5 m, t = 0.005 m, C = 0.5, $R_x = R_y$ = 10, (for spherical shell), α = 0.5, β = 0.5 and the material properties are assumed as E_1 = 141 GPa, E_2 = 9.23 GPa, $G_{12} = G_{13}$ = 5.95 GPa, G_{23} = 2.96 GPa, ρ = 1580 Kg/m^3, v = 0.3. Table 1 presents the non-dimensional buckling loads for the simply supported singly-curved cylindrical composite (0°/90°) panel for different b/R_y ratios (Baharlou and Leissa, 1987). Table 2 presents the convergence study of non-dimensional fundamental natural frequencies of three layered graphite-epoxy untwisted composite plates (Qatu and Leissa, 1991). A close agreement with benchmarking results are obtained in conjunction to (4 × 4), (8 × 8) and (10 × 10) mesh

1989). It can be noted here that, analysis of small constituent components is worthwhile and insightful to understand the structural behaviour of larger structures. For example, fuselage of aircraft consists of a cylindrical shell stiffened by circumferential frames and longitudinal stringers. Tests on full scale structure showed that adjacent panels across a frame vibrate independently of one another, with the frames acting as rigid boundaries (Clarson and Ford, 1962). Hence, in compliance of the same, the present study considers a simple example problem of a small component of laminated composite curved shells as a representative case to map the zone of dynamic instability due to stochastic variations on input parameters wherein the moving least square (MLS) model is employed to reduce the computational time and cost compared to Monte Carlo Simulation (MCS). However, in future, an extended work of the present study can be carried out to deal with the role of components in the overall stability of the whole large complex structural system.

Table 1 Non-dimensional buckling loads for the simply supported singly-curved cylindrical composite (0°/90°) panel with a = 0.25 m, b = 0.25 m, t=0.0025 m, a/R_x = 0, $E_1 = 2.07 \times 10^{11}$ N/m^2, $E_2 = 5.2 \times 10^9$ N/m^2, $G_{12} = 2.7 \times 10^9$ N/m^2, $\nu_{12} = 0.25$.

Structure	b/R_y=0.1	b/R_y=0.2	b/R_y=0.3
Present method	17.612	32.5027	57.117
Baharlou and Leissa (1987)	17.49	32.17	56.62

The moving lease square based approach is validated with original Monte Carlo simulation considering random variations of input parameters within upper and lower bounds (tolerance zone). Figure 3 presents the scatter plot which establishes the accuracy of present MLS model with respect to original finite element model corresponding to stochastic first buckling load for combined variation of ply-orientation angle, radius of curvatures, material

= 0.5, E_1 = 138 GPa, E_2 = 8.96 GPa, G_{12} = 7.1 GPa, v_{12} = 0.3.

Structure	Present FEM (4 × 4)	Present FEM (8 × 8)	Present FEM (10 × 10)	Qatu and Leissa (1991)
Plate	0.4600	0.4581	0.4577	0.4607
Spherical Shell	1.3507	1.2977	1.2941	1.3063

Table 3 Non-dimensional fundamental frequencies [$\omega=\omega_n\ a^2\ \sqrt{(\rho/E_2t^2)}$] for the simply supported four layered cross-ply (0°/90°/90°/0°) composite with E_{11}/E_{22} = 25, G_{23} = 0.2E_{22}, G_{12} = G_{13} = 0.5E_{22}, v_{12} = 0.25.

Analysis	a/t=100		a/t=10	
	Plate	Spherical (R/b=1)	Plate	Spherical (R/b=1)
Present FEM	15.187	126.320	12.228	16.146
Reddy (1984)	15.184	126.330	12.226	16.172
Chandrashekhara (1989)	15.195	126.700	12.233	16.195

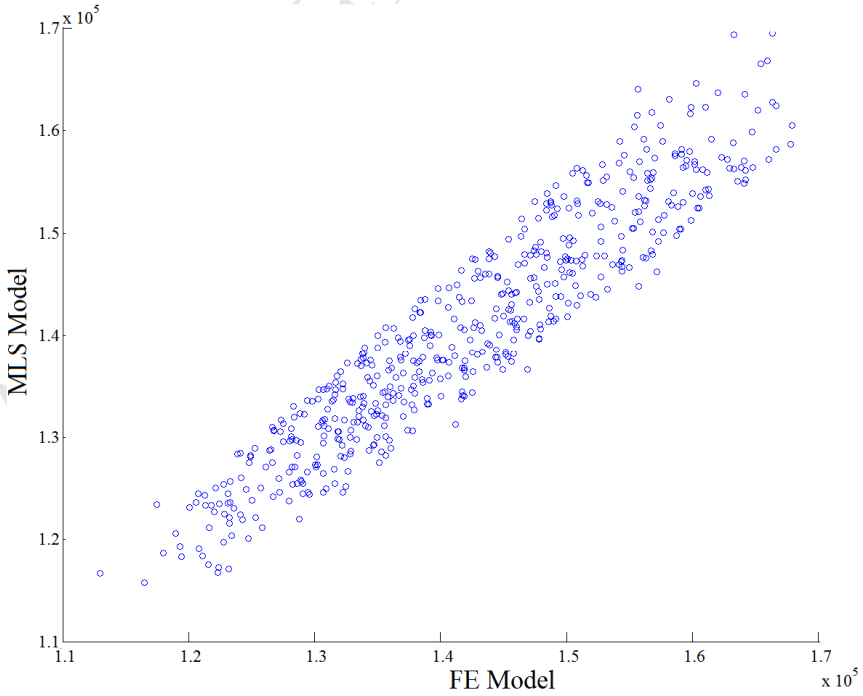

Fig. 3 Scatter plot for stochstic buckling loads corresponding to FE model and MLS model

is used to determine the first stochastic buckling load and resonance frequencies corresponding to given values of input variables, instead of time-consuming deterministic finite element analysis. The probability density function is plotted as the benchmark of bottom line results. The variations of material properties, load intensity and factors are scaled in the range between the lower and the upper limit (tolerance limit) as ±10% with respective mean values while for ply orientation angle as within ±5º fluctuation (as per standard of composite manufacturing industry) with respective deterministic values. Due to paucity of space, only a few important representative results are furnished.

A sample size of 64 is considered in case of individual variation of stochastic input parameters while due to higher number of input variables for combined random variation, the subsequent sample size of 512 is found to meet the convergence criteria in the present MLS method. The sampling size of 10,000 is considered for direct MCS with 10,000 finite element (FE) iteration. In contrast, comparatively much lesser number of actual FE iteration (equal to number of design points required to construct the surroagte model) is carried out in case of MLS method. The surrogate model is formed employing MLS method, on which the full sample size of direct MCS is conducted. Hence, the computational time and effort expressed in terms of FE calculation is significantly reduced compared to full scale direct MCS. This provides an efficient and economic way to simulate the uncertainties in buckling load and resonance frequencies (both upper bound and lower bound) for dynamic stability analysis. The scatter plot is also presented for validation of the present MLS model with original FE model with respect to resonance frequencies (fundamental) of lower bound [Figure 4(a)] and upper bound [Figure 4(b)] corresponding to combined variation of ply-orientation angle, radius of curvatures, material properties, load, load factors (both static and dynamic). The

interval boundaries (95%, 97% and 99%) for mean and standard deviation of buckling load are shown in Table 4 for samples of direct MCS and MLS model.

Table 4 Confidence interval boundaries for mean and standard deviation of buckling load (KN/m) for samples of direct MCS and MLS model

Confidence interval (%)		MLS		MCS	
		Mean	SD	Mean	SD
95	Min	1.35240×10^{5}	1.64351×10^{4}	1.35869×10^{5}	1.48764×10^{4}
	Max	1.36893×10^{5}	1.68972×10^{4}	1.36460×10^{5}	1.52946×10^{4}
97	Min	1.35205×10^{5}	1.64110×10^{4}	1.35837×10^{5}	1.48545×10^{4}
	Max	1.36928×10^{5}	1.69226×10^{4}	1.36492×10^{5}	1.53176×10^{4}
99	Min	1.35137×10^{5}	1.63645×10^{4}	1.35776×10^{5}	1.48124×10^{4}
	Max	1.36996×10^{5}	1.69718×10^{4}	1.36553×10^{5}	1.53621×10^{4}

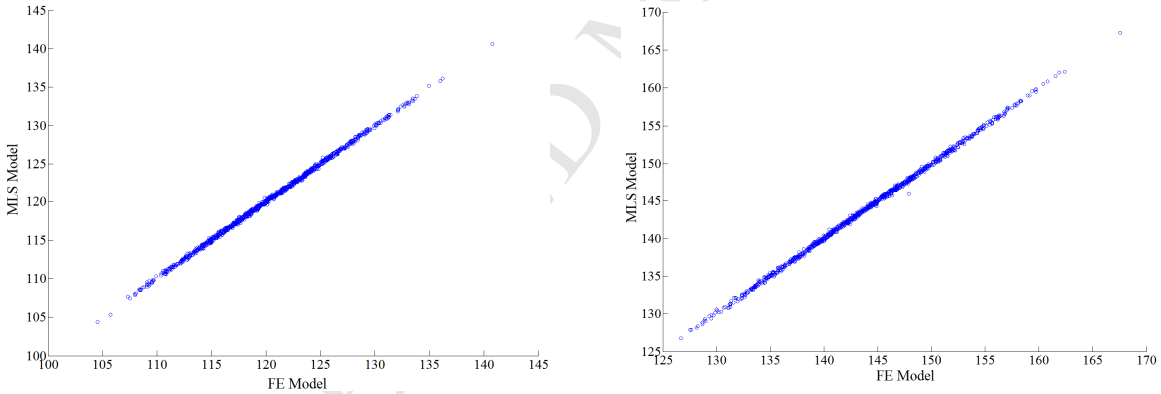

(a) (b)

Fig. 4 Scatter plot for (a) lower bound and (b) upper bound of fundamental resonance frequencies corresponding to combined variation

The MLS model is validated extensively for different laminate configurations as well as different forms of stochasticity (individual and combined) so that the computationally efficient surrogate is ensured to obtain accurate results in the uncertainty analysis. The combined variations of stochastic input parameters for both MCS as well as present MLS

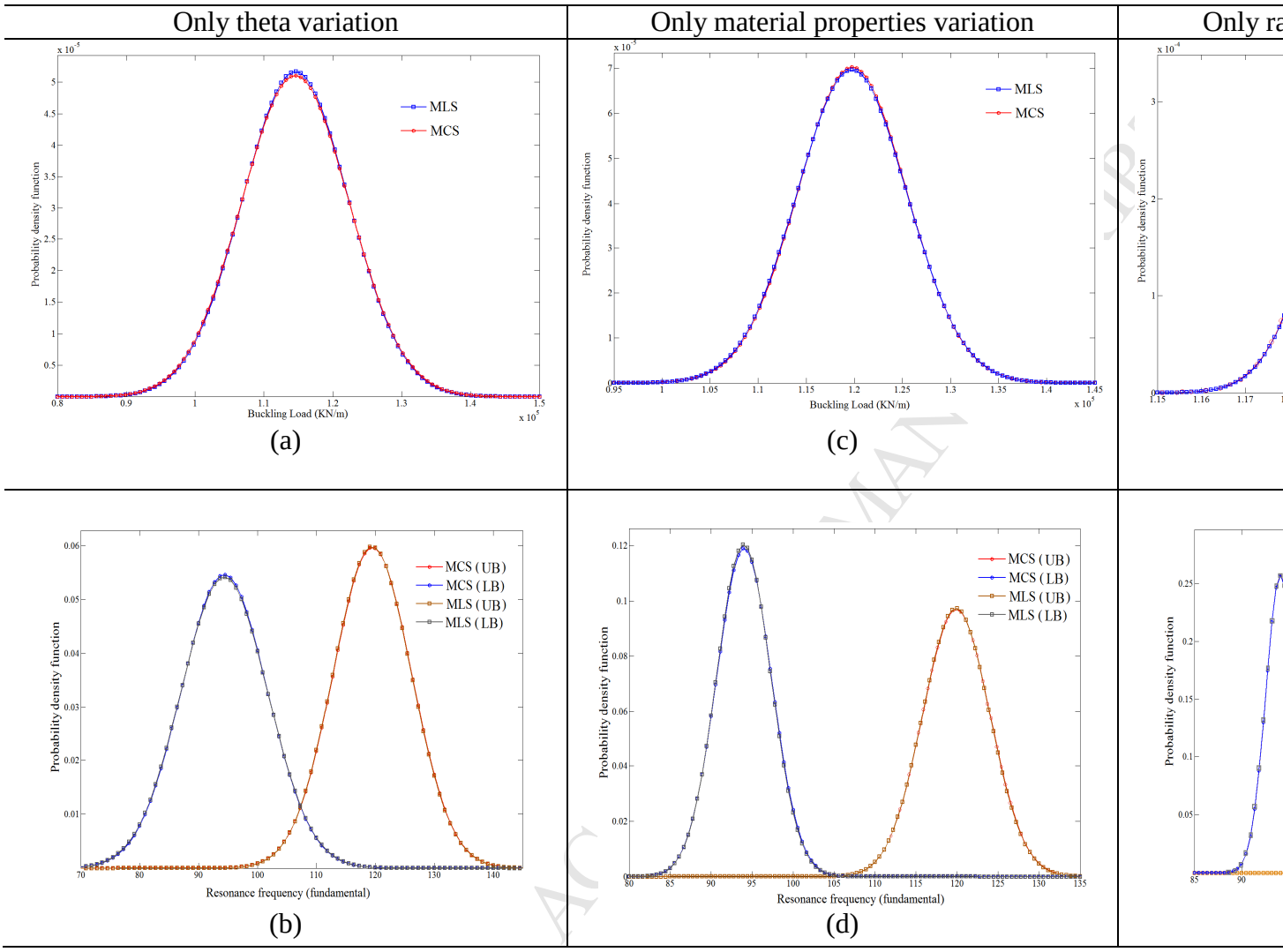

Fig. 5 Probability density function obtained by original Monte Carlo Simulation (MCS) and Moving Least Squa load (first) and fundamental resonance frequencies [Upper Bound(UB), Lower Bound(LB)] due to individual material properties and radius of curvatures for angle –ply (45°/-45°/45°/-45°) composite spherical shells

Laminate	Buckling Load (first)	Resonance frequencies (
Angle–ply (45°/-45°/ 45°/-45°)	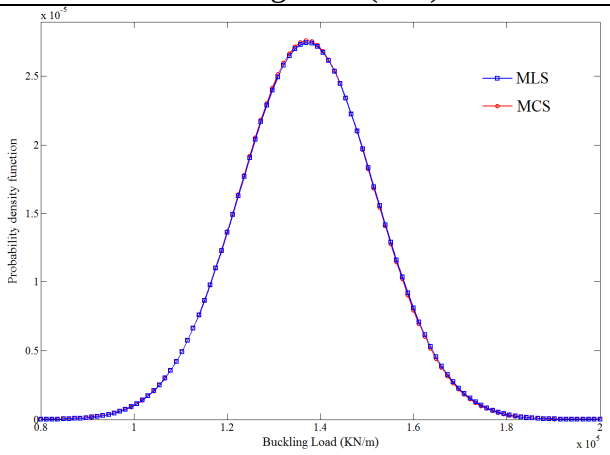 (a)	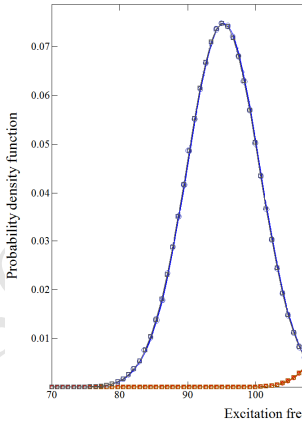 (b
Cross–ply (0°/90°/ 0°/90°)	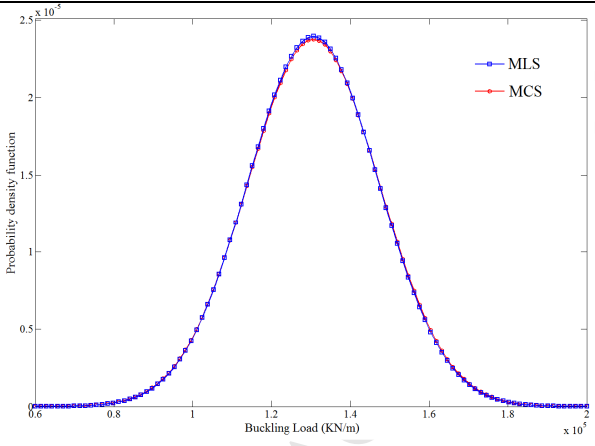 (c)	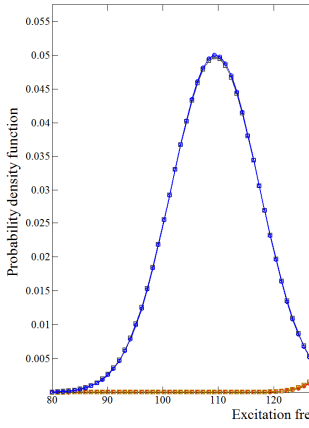 (d

Fig. 6 Probability density function obtained by original Monte Carlo Simulation (MCS) and Moving Least Square load (first) and (b) fundamental resonance frequencies [Upper Bound(UB), Lower Bound(LB)] due to combin angle–ply and cross-ply composite spherical shells

Table 5 Stochastic buckling load (first) and resonance frequencies (first and second) with error due to individua supported angle-ply (45°/-45°/45°/-45°) composite spherical shells considering L=1 m, b=0.5 m, t=0.005 m, c=(G_{12}=G_{13}=5.95 GPa, G_{23}=2.96 GPa, ρ=1580 Kg/m^3, v=0.3

Para-meter	Value	Buckling Load (first)			Resonance frequency (First)						Reso	
		MCS	MLS	Err %	Upper bound			Lower bound			Upper bou	
					MCS	MLS	Err %	MCS	MLS	Err %	MCS	MLS
$\theta(\tilde{\omega})$	Max	128291.9	127596.5	0.54	137.13	136.76	0.27	114.56	115.37	-0.71	154.45	154.6
	Min	88701.2	85767.6	3.31	102.14	101.13	0.99	77.68	76.36	1.70	126.19	124.6
	Mean	114559.3	114586.8	-0.02	119.50	119.45	0.04	94.37	94.35	0.02	143.71	143.6
	SD	7812.6	7718.3	1.21	6.68	6.66	0.30	7.30	7.36	-0.82	4.83	4.8
$R(\tilde{\omega})$	Max	122779.8	122735.2	0.04	123.17	123.12	0.04	97.61	97.59	0.02	153.27	153.1
	Min	117567.8	117573.0	0.00	117.25	117.26	-0.01	91.12	91.12	0.00	135.49	135.4
	Mean	119910.8	119919.8	-0.01	119.94	119.96	-0.02	94.08	94.09	-0.01	144.22	144.2
	SD	1202.1	1199.9	0.18	1.41	1.40	0.71	1.55	1.54	0.65	3.74	3.7
$P(\tilde{\omega})$	Max	131650.3	131442.9	0.16	131.05	130.91	0.11	103.32	103.17	0.15	157.51	157.2
	Min	108278.9	108146.1	0.12	109.54	110.03	-0.45	85.33	85.43	-0.12	131.57	132.3
	Mean	119787.4	119748.1	0.03	119.92	119.89	0.03	94.01	93.98	0.03	144.11	144.0
	SD	5678.4	5728.4	-0.88	4.11	4.10	0.24	3.35	3.31	1.19	5.10	5.0
$F(\tilde{\omega})$	Max	157639.4	157447.1	0.12	120.36	120.38	-0.02	96.25	96.28	-0.03	143.98	144.0
	Min	119790.2	119692.4	0.08	119.81	119.79	0.01	93.94	93.92	0.02	143.45	143.4
	Mean	137767.5	137644.7	0.09	120.08	120.08	-0.01	95.11	95.11	0.00	143.71	143.7
	SD	12653.6	12272.1	3.01	0.27	0.27	0.00	0.89	0.87	2.25	0.26	0.2
$\{\theta,R,P,F,\alpha,\beta\}$	Max	177886.5	180808.1	-1.64	140.77	139.61	0.82	114.082	117.94	3.38	169.30	165.8
	Min	101954	101032.5	0.90	103.79	104.23	-0.42	77.42	78.28	-1.11	124.71	124.7
	Mean	137164.4	137238.2	-0.05	120.20	120.18	0.02	95.27	95.28	-0.01	144.03	143.9
	SD	14468.9	11919.0	17.62	5.40	5.44	-0.74	5.32	5.23	1.69	6.58	6.60

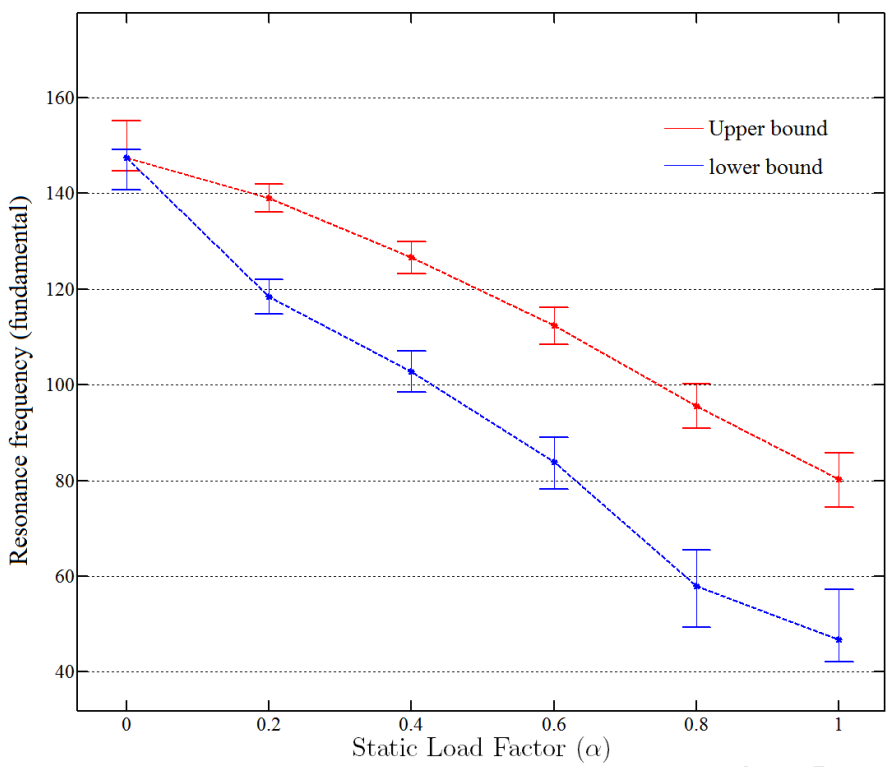

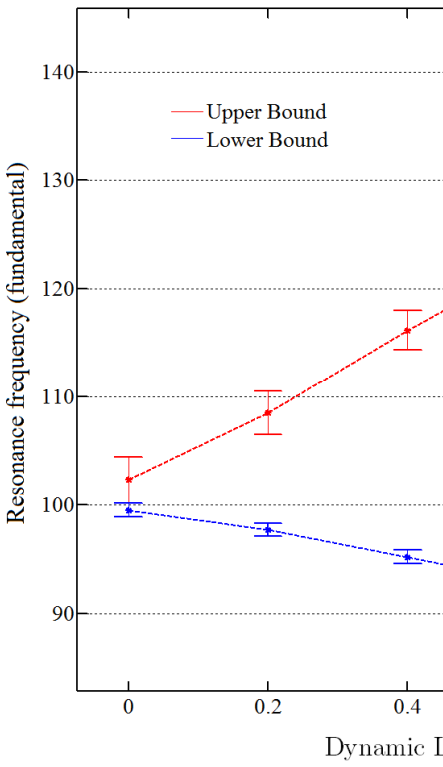

(a)

Fig. 7 Effect of static load factor and dynamic load factor on stochastic resonance frequencies (fundamental) orientation angle, radius of curvatures, material properties, loading for simply supported angle-ply (45°/-45°/45°/-

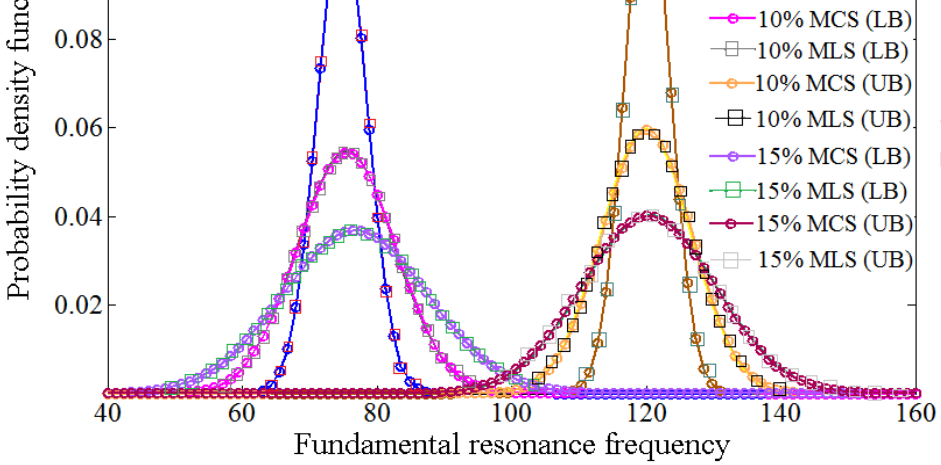

Fig. 8 Effect of percentage variation (5%, 10% and 15%) for combined variations of input parameters on resonance frequencies (fundamental) for simply supported angleply (45°/-45°/45°/-45°) composite spherical shells

method are carried out corresponding to both angle-ply (45°/-45°/45°/-45°) and cross-ply (0°/90°/0°/90°) composite spherical shells. Due to random variation of input parameters, the elastic stiffness of the laminated composite plate is found to be varied, which in turn influence the stochastic output irrespective of laminate configuration. Table 5 presents the comparative results of Monte Carlo simulation (MCS) and present MLS method for first buckling load and resonance frequencies (upper bound and lower bound) due to individual and combined variations of ply-orientation angle, radius of curvatures, material properties, intensity of load and load factors of a simply supported angle-ply (45°/-45°/45°/-45°) composite shallow spherical shells. The influence of static load factor and dynamic load factor on stochastic resonance frequencies due to combined variation of ply-orientation angle, radius of curvatures, material properties, loading for angle-ply (45°/-45°/45°/-45°) composite spherical shells are furnished in Figure 7. It is observed that the width of the instability zone increases with the increase of static and dynamic load factors. Based on the rate of increment of the region of instability, it can be inferred that the dynamic load factor (β) is more sensitive

for higher degree of variations in the stochastic input parameters, three different degree of stochasticities are considered: 5%, 10% and 15% variations in the stochastic input parameters with respect to their respective deterministic values. Figure 8 presents the validation in resonance frequencies (fundamental) using MLS model corresponding to different degree of stochasticities (5%, 10% and 15%) for combined variation of input parameters considering simply supported angle-ply spherical shells. The figure clearly depicts the increase in sparsity of resonance frequency (fundamental) due to increase in percentage of varitions of random input parameters. The figure also affirms that the proposed MLS based uncertainty quantification algorithm for composites produces quite satisfactory results for different degree of stochasticities in input parameters with respect to direct Monte Carlo simulations.

Depending on the geometry of doubly curved shells, a comparative study is carried out for cylindrical, hyperbolic paraboloid and spherical shells as furnished in Figure 9 for both stochastic buckling load and random resonance frequencies (fundamental) due to combined variation of for cross-ply (0°/90°/0°/90°) composite shells. The zone of resonance frequencies (fundamental) maps the different instability regions for different shell geometries. It is observed that the resonance frequency (fundamental) decreases with reduction of curvatures from spherical shell to hyperbolic paraboloid shells while single cylindrical shell shows the least stiffness compared to the other two. In order to address the influence of degree of shallowness (R_x/a = R_y/b = 5, 10, 20) of the doubly curved shells, a spherical shell is considered to portray the instability regions as furnished in Figure 10. It is identified that there is an increase of instability resonance frequencies with the decrease in radius of curvature along x and y directions (i.e., R_x and R_y values). The significant effects of degree of orthotropy on stochastic buckling load and resonance frequency (fundamental) due to

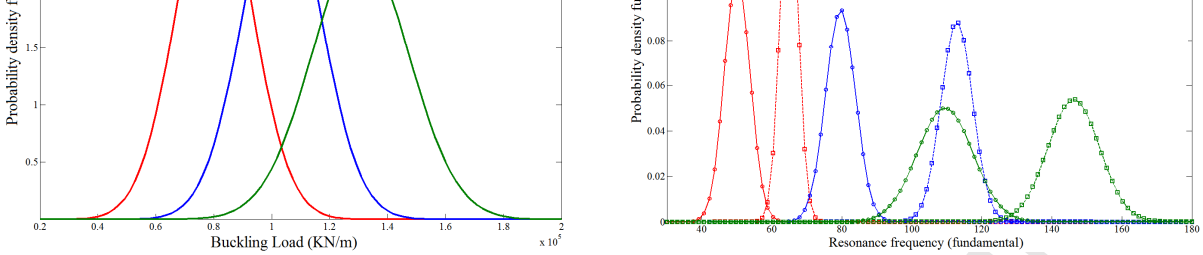

(a) (b)

Fig. 9 Effect of shell geometry (Cylindrical, Hyperbolic paraboloid and Spherical) on stochastic (a) buckling load (first) and (b) resonance frequencies (fundamental) due to combined variation of for simply supported cross-ply (0°/90°/0°/90°) composite curved shells

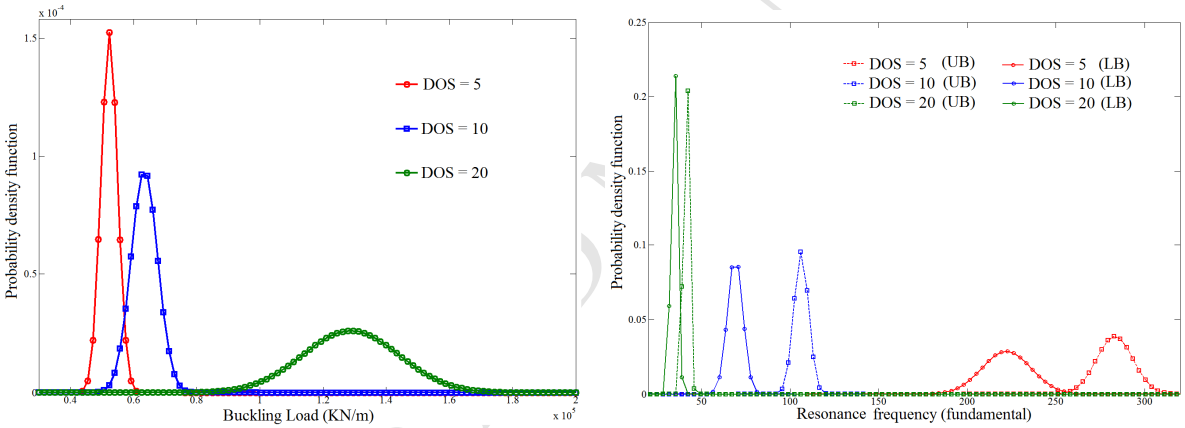

(a) (b)

Fig. 10 Effect of degree of shallowness (DOS) (R_x/a=R_y/b) on stochastic (a) buckling load (first) and (b) resonance frequencies (fundamental) due to combined variation of for simply supported cross-ply (0°/90°/0°/90°) composite spherical shells

combined variation of ply-orientation angle, radius of curvatures, material properties, loading for cross-ply composite spherical shells are furnished in Figure 11. As the static parameter is increased, the dynamic instability zone tend to shift towards lower frequencies and become stipper. The effect of degree of orthotropy is studied for E_1/E_2 ratio = 15, 30, 45, by randomizing the other parameters. The study shows an increase of random resonance

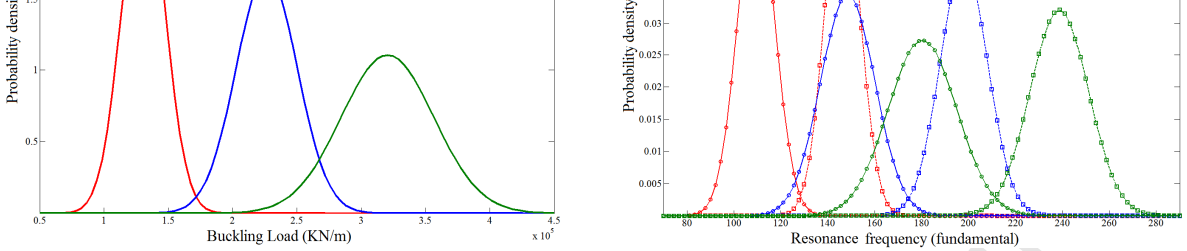

(a) (b)

Fig. 11 Effect of degree of orthotropy on stochastic (a) buckling load (first) and (b) resonance frequencies (fundamental) due to combined variation for simply supported cross-ply (0°/90°/0°/90°) composite spherical shells

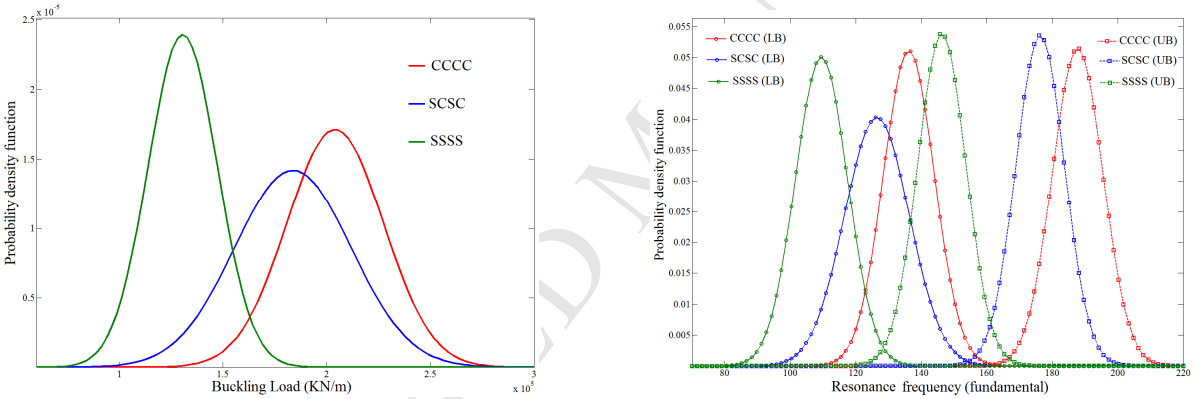

(a) (b)

Fig. 12 Effect of boundary end condition (CCCC, SCSC, SSSS) on stochastic (a) buckling load and (b) resonance frequency (fundamental) due to combined variation for cross-ply (0°/90°/0°/90°) composite spherical shells

frequencies due to increase in degree or orthotropy. The boundary conditions of the composite shells are observed to have a significant influence on the dynamic instability regions. The influence of different boundaries (CCCC, SCSC, SSSS where C – clamped, S-Simply supported) is investigated for stochastic buckling load and first resonance frequencies (lower and upper bounds) due to combined variation of ply-orientation angle, radius of curvatures, material properties, loading for cross-ply composite spherical shells by

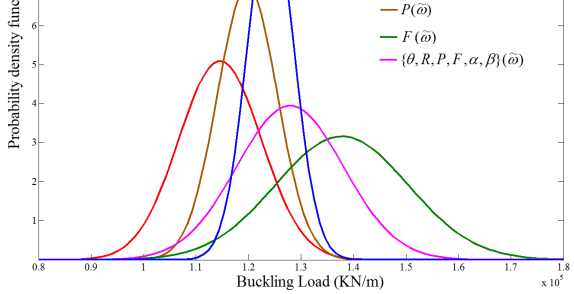

Fig. 13 Stochastic buckling load for combined variation for simply supported cross-ply spherical shells

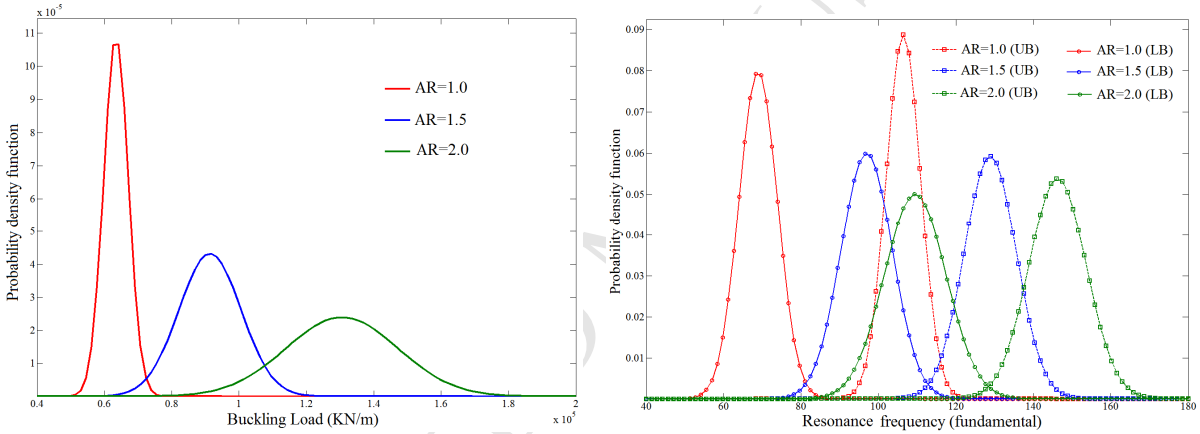

(a) (b)

Fig.14 Effect of aspect ratio (AR) on stochastic (a) buckling load and (b) resonance frequencies (fundamental) for combined variation for simply supported cross-ply spherical shells

probability density function as furnished in Figure 11. This study shows that the stochastic resonance frequencies are found minimum for simply supported and maximum for clamped edges due to the restraint at the edges while SCSC boundary condition is found to be intermediate for both stochastic buckling load as well as zone of resonance frequencies.

The effect of individual variations and combined variation of different random parameters for angle-ply composite spherical shells on stochastic first buckling load are

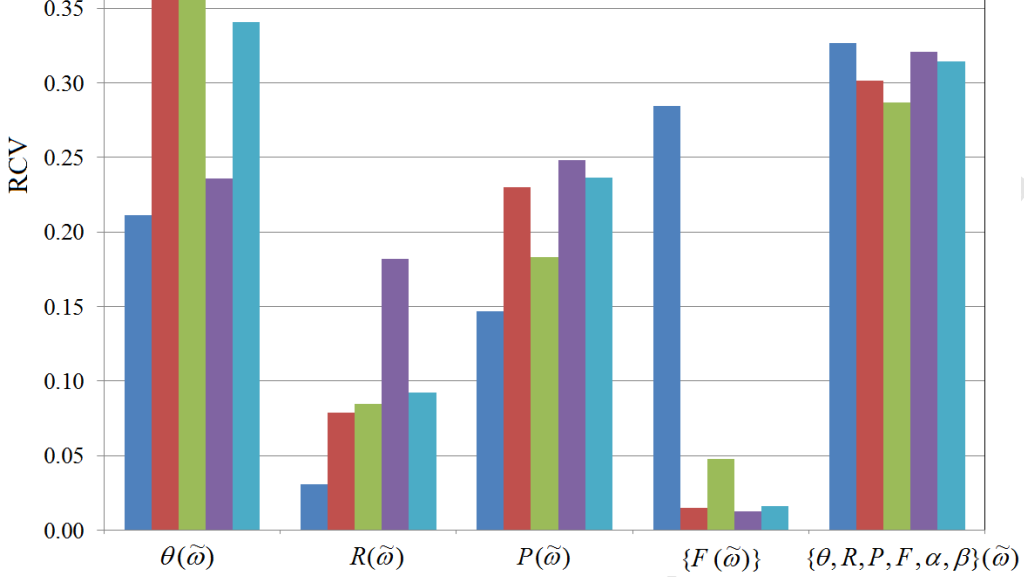

Fig. 15 Relative coefficient of variance (RCV) of buckling load and first resonance frequencies (FRF) and second resonance frequencies (SRF) due to individual variation of ply orientation angle, radius of curvatures, material properties, loading and combined variation for simply supported angle-ply (45°/-45°/45°/-45°) composite spherical shells.

furnished in Figure 13 wherein the maximum sparsity of buckling load is observed for only variation of load-intensity among all the individual parameters. Figure 14 represents the influence of aspect ratio (AR = a/b) on stochastic buckling load and resonance frequency (fundamental) due to combined variation of ply-orientation angle, radius of curvatures, material properties, loading for cross-ply composite spherical shells. Because of the shear deformation, it is found that the width of instability region narrows down. It is also found that as the aspect ratio (a/b) increases, the resonance frequencies also increase and the width of instability zone becomes wider. In the present study, the relative coefficient of variance (RCV) (normalized mean to standard deviation ratio) due to individual and combined variations is quantified for angle-ply laminate as furnished in Figure 15. On the basis of individual variation of input parameters, ply orientation angle is found to be comparatively

7. Conclusions

This study illustrates an efficient stochastic dynamic stability analysis of laminated composite curved panels considering non-uniform partial edge loading. The ranges of variation in first stochastic buckling load and fundamental resonance frequencies are analyzed considering both individual and combined stochasticity of input parameters. Novelty of the present study includes an efficient stochastic dynamic stability analysis with random non-uniform loading. Moving least square method is employed in conjunction with stochastic finite element analysis following a non-intrusive approach to achieve the computational efficiency. After utilizing the surrogate modelling approach, the number of finite element simulations is found to be significantly reduced compared to original Monte Carlo simulation without compromising the accuracy of results. The computational time is reduced to (1/157) times (for individual variation) and (1/20) times (for combined variation) of Monte Carlo simulation. The stochastic instability regions are found to shift to lower frequencies with increase in static load factor showing wider random instability regions indicating destabilization effect on the dynamic stability characteristics of composite spherical shells. It is observed that the zone of stochstic instability has significant influence due to variation in degree of orthotropy, aspect ratio and boundary condition. The width of stochstic instability region increases with the increase of degree of orthotropy and aspect ratio. The ply orientation angle is found to be most sensitive, while the least sensitive parameters are observed as loading parameter (for resonance frequencies) and radius of curvatures (for buckling load) compared to other parameters considered in this analysis.

Laminated composites being a complex structural form and susceptible to different forms of uncertainty, the compound effects of stochastic time varying loading and structural

has significant impact on dynamic instability of composite shell structures and thus such sensitive parameters are to be considered in design for operational safety and serviceabilty point of view. The numerical results obtained in this study provide a comprehensive idea for design and control of laminated composite curved pamels. The effiecient moving least square based approach of uncertainty quantification can be extended further to other computationally intensive analyses of composite structures.

Acknowledgements

TM acknowledges the financial support from Swansea University through the award of Zienkiewicz Scholarship. SA acknowledges the financial support from The Royal Society of London through the Wolfson Research Merit award.

References

Andrzej T., Ratko P., Predrag K., 2011. Influence of transverse shear on stochastic instability of symmetric cross-ply laminated plates, *Probabilistic Engineering Mechanics*, 26, 454–460.

Baharlou B., Leissa A.W., 1987. Vibration and buckling of generally laminated composite plates with arbitary edge conditions, *Int. J. Mechanical Sciences*, 29(8), 545–555.

Bathe K.J., 1990. *Finite Element Procedures in Engineering Analysis*, PHI, New Delhi.

Bert C.W., Birman V., 1988. Parametric instability of thick orthotropic circular cylindrical shells, *Acta Mechanica*, 71, 61–76.

Bolotin V.V., 1964. The dynamic stability of elastic system, San Francisco: Holden-Day.

Breitkpf P., Naceur H., Rassineux A., Villon P., 2005. Moving least squares response surface approximation: formulation and metal forming applications, *Computers and Structures*, 83, 1411-1428.

Chandrashekhara, K., 1989. Free vibrations of anisotropic laminated doubly curved shells, *Computers and Structures*, 33, 435–440.

Chaudhuri R.A., Abuarja K.R., 1988. Extract solution of shear flexible doubly curved antisymmetric angle ply shells, *Int.J.Engineering Sciences*, 26(6), 587–604.

Chen L.W., Yang J.Y., 1990. Dynamic stability of laminated composite plates by the finite element method, *Computers & Structures*, 36(5), 845–851.

Choi S., Grandhi R.V., Canfield R.A., 2004. Structural reliability under non-gaussian stochastic behavior, *Computers & Structures*, 82, 1113-1121.

Clarson B.L, Ford R.D., 1962. The response of a typical aircraft structure to jet noise, *Journal of the Royal Aeronautical Society*, 66, 31-40.

Composite Structures, 171 227–250

Dey S., Mukhopadhyay T., Khodaparast H. H., Adhikari S., 2016b. Fuzzy uncertainty propagation in composites using Gram-Schmidt polynomial chaos expansion, *Applied Mathematical Modelling*, 40 (7–8) 4412–4428

Dey S., Mukhopadhyay T., Khodaparast H. H., Adhikari S., 2016f. A response surface modelling approach for resonance driven reliability based optimization of composite shells, *Periodica Polytechnica - Civil Engineering*, 60 (1) 103–111

Dey S., Mukhopadhyay T., Khodaparast H. H., Kerfriden P., Adhikari S., 2015c. Rotational and ply-level uncertainty in response of composite shallow conical shells, *Composite Structures*, 131 594–605

Dey S., Mukhopadhyay T., Naskar S., Dey T. K., Chalak H. D., Adhikari S., 2018. Probabilistic characterization for dynamics and stability of laminated soft core sandwich plates, *Journal of Sandwich Structures & Materials*, DOI: 10.1177/1099636217694229

Dey S., Mukhopadhyay T., Sahu S. K., Adhikari S., 2016e. Effect of cutout on stochastic natural frequency of composite curved panels, *Composites Part B: Engineering*, 105, 188–202

Dey S., Mukhopadhyay T., Sahu S.K., Li G., Rabitz H., Adhikari S., 2015d. Thermal uncertainty quantification in frequency responses of laminated composite plates, *Composites Part B: Engineering*, 80 186–197

Dey S., Mukhopadhyay T., Spickenheuer A., Adhikari S., Heinrich G., 2016c. Bottom up surrogate based approach for stochastic frequency response analysis of laminated composite plates, *Composite Structures*, 140 712–727

Dey S., Mukhopadhyay T., Khodaparast H. H., Adhikari S., 2015b. Stochastic natural frequency of composite conical shells, *Acta Mechanica*, 226 (8) 2537-2553

Dey S., Naskar S., Mukhopadhyay T., Gohs U., Spickenheuer A., Bittrich L., Sriramula S., Adhikari S., Heinrich G., 2016a. Uncertain natural frequency analysis of composite plates including effect of noise – A polynomial neural network approach, *Composite Structures*, 143 130–142

Dey S., Mukhopadhyay T., Spickenheuer A., Gohs U., Adhikari S., 2016d. Uncertainty quantification in natural frequency of composite plates - An Artificial neural network based approach, *Advanced Composites Letters*, 25(2) 43–48

functionally graded truncated conical shells surrounded on elastic foundations, *European Journal of Mechanics - A/Solids*, 50, 120–131.

Evan-Iwanowski R.M., 1965. On the parametric response of structures, *Applied Mechanics Review*, 18, 699–702.

Gadade A.M., Lal A., Singh B.N., 2016. Accurate stochastic initial and final failure of laminated plates subjected to hygro-thermo-mechanical loadings using Puck's failure criteria, *International Journal of Mechanical Sciences*, 114, 177-206.

Ganapathi M., Boisse P., Solaut D., 1999. Non-linear dynamic stability analysis of composite laminates under periodic in-plane loads, *International Journal for Numerical Methods in Engineering*, 46, 943–956.

Guilleminot J., Soize C., Kondo D., Binetruy C., 2008. Theoretical framework and experimental procedure for modelling mesoscopic volume fraction stochastic fluctuations in fiber reinforced composites, *Int. J. of Solids and Structures*, 45(21), 5567-5583.

Iwatsubo T., Saigo M., Sugiyama Y., 1973. Parametric instability of clamped-clamped and clamped-simply supported columns under periodic axial load, *Journal of Sound and Vibration*, 30, 65–77.

Kaminski M., 2013. The stochastic perturbation method for computational mechanics. John Wiley & Sons.

Kang Soo-Chang, Koh Hyun-Moo, Choo Jinkyo F., 2010. An efficient response surface method using moving least squares approximation for structural reliability analysis, *Probabilistic Engineering Mechanics*, 25, 365-371.

Kim N., Jeon C.K., Lee J., 2013. Dynamic stability analysis of shear-flexible composite beams, *Archive of Applied Mechanics*, 83(5), 685-707.

Kochmann D.M., Drugan W.J., 2009. Dynamic stability analysis of an elastic composite material having a negative-stiffness phase, *Journal of the Mechanics and Physics of Solids*, 57(7), 1122–1138.

Lan X., Feng Z., Lv F., 2014. Stochastic principal parametric resonances of composite laminated beams, *Shock and Vibration*, doi: 10.1155/2014/617828

Lancaster P., Salkauskas K., 1981. Surfaces generated by moving least squares methods, *Mathematics of Computation*, 37(155), 141-158.

Meirovitch L., 1992. Dynamics and Control of Structures, John Wiley & Sons, NY.

Meng-Kao Y., Yao T.K., 2004. Dynamic instability of composite beams under parametric excitation, *Composites Science and Technology*, 64, 1885–1893.

Moorthy J., Reddy J.N., 1990. Parametric instability of laminated composite plates with transverse shear deformation, *International Journal of Solids and Structures*, 26(7), 801–811.

Mukhopadhyay T., Chakraborty S., Dey S., Adhikari S., Chowdhury R., 2017. A critical assessment of Kriging model variants for high-fidelity uncertainty quantification in dynamics of composite shells, *Archives of Computational Methods in Engineering*, 24(3) 495–518

Mukhopadhyay T., Dey T.K., Dey S., Chakrabarti A., 2015. Optimization of fiber reinforced polymer web core bridge deck - A hybrid approach, *Structural Engineering International*, 24(2), 173-183.

Naskar S., Mukhopadhyay T., Sriramula S., Adhikari S., 2017. Stochastic natural frequency analysis of damaged thin-walled laminated composite beams with uncertainty in micromechanical properties, *Composite Structures*, 160 312–334

Park I., Grandhi R.V., 2014. A Bayesian statistical method for quantifying model form uncertainty and two model averaging techniques, *Reliability Engineering & System Safety*, 129, 46-56.

Patel S.N., Datta P.K., Sheikh A.H., 2009. Parametric study on the dynamic instability behavior of laminated composite stiffened plate, *Journal of Engineering Mechanics*, 135(11), 1331-1341.

Qatu M.S., Leissa A.W., 1991. Natural frequencies for cantilevered doubly curved laminated composite shallow shells, *Composite Structures*, 17, 227–255.

Ratko P., Predrag K., Snezana M., Ivan P., 2012. Influence of rotatory inertia on dynamic stability of the viscoelastic symmetric cross-ply laminated plates, *Mechanics Research Communications*, 45, 28– 33.

Reddy J.N., 1984. Exact solutions of moderately thick laminated shells, *Journal of Engineering Mechanics*, 110, 794–809.

Saraviaa M., Machadoa S.P., Cortíneza V.H., 2011. Free vibration and dynamic stability of rotating thin-walled composite beams, *European Journal of Mechanics - A/Solids*, 30 (3), 432–441.

Sarrouy E., Dessombz O., Sinou J.J., 2013. Stochastic study of a non-linear self-excited system with friction, *European Journal of Mechanics - A/Solids*, 40, 1–10.

Sepe R., Luca A. De, Lamanna G., Caputo F., 2016. Numerical and experimental investigation of residual strength of a LVI damaged CFRP omega stiffened panel with a cut-out, *Composites Part B: Engineering*, 102, 38-56.

Shu C., Wu W.X., Ding H., Wang C.M., 2007. Free vibration analysis of plates using least-square-based finite difference method, *Computer Methods in Applied Mechanics and Engineering*, 196(7), 1330–1343.

Singha M.K., Daripa R., 2009. Non-linear vibration and dynamic stability analysis of composite plates, *Journal of Sound and Vibration*, 328, 541–554.

Wu Lanhe, Li Hua, Wang Daobi, 2005. Vibration analysis of generally laminated composite plates by the moving least squares differential quadrature method, *Composite Structures*, 68, 319–330.

Yao J.C., 1965, Nonlinear elastic buckling and parametric excitation of a cylinder under axial loads, *Journal of Applied Mechanics*, 32, 109–115.

Yeh M.K., Kuo Y.T., 2004. Dynamic instability of composite beams under parametric excitation, *Composites Science and Technology*, 64, 1885–1893.

3. Stochasticity in composite system properties (structural and material attributes) as well as loading is considered.

4. A surrogate based approach is adopted to achieve computational efficiency in the stochastic analysis.